Macromolecular Research

Article

DOI 10.1007/s13233-020-8090-4

www.springer.com/13233 pISSN 1598-5032 eISSN 2092-7673

Fabrication and Analysis of Long Fiber Reinforced Polypropylene Prepared *via* Injection Molding

Seon Yeong Park
Young Seok Song*

Department of Fiber System Engineering, Dankook University, Gyeonggi 16890, Korea

Received October 4, 2019 / Revised January 13, 2020 / Accepted February 9, 2020

Abstract: Fiber reinforcement leads to an improvement in mechanical properties of composites. In particular, long fiber thermoplastics (LFT) show more remarkable enhancement in the properties than short fiber thermoplastics (SFT). In this study, different fiber lengths, fiber loadings, and processing methods were considered to understand their effects on the physical properties more in-depth. It was found that significant breakage of fibers occurred during the screw based injection molding, which yielded a significant reduction in the properties. The orientation of fiber was observed experimentally and compared with the result of numerical simulation.

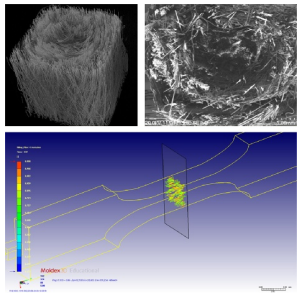

Keywords: polypropylene, glass fiber, carbon fiber, long fiber reinforced thermoplastics, injection-molding.

1. Introduction

At present, composites manufacturing is being actively researched for various applications such as electronics, automobiles, ships and airplanes.[1-6] In particular, fiber reinforced thermoplastics that use a variety of fibers as a filler have attracted substantial attention and are increasingly employed. since the use of fibers in composites can enhance physical properties such as strength, rigidity, and modulus. In addition, since the fibers have a high aspect ratio, they have good adhesion with the matrix. The properties of fiber reinforced composites depend on the type of fiber, fiber length, and fiber loading. For long fiber thermoplastics (LFTs), since the length of the fiber is relatively long the adhesion with the matrix is increased, and a network structure of fibers can be formed. As a result, the strength of LFTs can be greatly increased compared to that of short fiber thermoplastics (SFTs). Furthermore, since LFTs are easy to process and are relatively inexpensive,[7] they show a potential for replacing metals.

Among reinforcing fibers, glass fiber (GF) is the most widely used for the fiber reinforced composites.[8,9] Because glass fiber reinforced thermoplastics have excellent durability, impact resistance, corrosion resistance, and low thermal conductivity, they are applied for various products such as buildings, sports equipment, cars, aircraft parts, and so on. On the other hand, carbon fiber (CF) is also widely employed because of its good mechanical properties.[10-12] Although CF is more expensive than GF, it can reduce the weight of final products because of its relatively low density.[13] Polypropylene (PP), a typical commodity polymer shows good impact strength, heat resistance, and chemical resistance. Moreover, it is inexpensive and can be recycled relatively easily.[14,15] Hence, PP is being used as a matrix of fiber reinforced composites.

The pultrusion process is a method in which fibers are impregnated with a resin and then molded by pulling.[16,17] It can manufacture products with uniform cross-sectional shape, such as rods and pipes, maximizing the fiber impregnation. In the case of LFTs, the pultrusion process can be applied to produce pellets for the following polymer processing.[18]

Injection molding is one of the important polymer processing methods. In the injection-molding process, polymer is heated, the fluidized polymer is injected into the mold, then the polymer is cooled, solidified, and molded.[19,20] It can mass-produce polymeric and/or composite parts with various sizes and shapes, such as automobile body panels at low cost. On the other hand, reinforcing fibers undergo severe damage in length when using screw type injection molding machines.

In this study, we investigated fiber reinforced composites. The pellets for LFTs were prepared using the pultrusion process and used for injection molding. Two different types of injection moldings, screw-type and plunger type injection moldings were considered to analyze the damage of fiber length after processing. The effects of fiber length and content on the physical properties such as mechanical, thermal, and rheological properties of LFTs were examined. The morphological analysis of the composites was carried out using scanning electron microscopy (SEM) and micro-computer tomography (μ-CT). In addition, the fiber orientation of fibers in the composites was simulated numerically and compared with experimental results.

Acknowledgments: This work was supported by GRRC program of Gyeonggi Province (GRRC Dankook2016–B03). In addition, this research was supported by Basic Science Research Program through the National Research Foundation of Korea (NRF) funded by the Ministry of Education (2018R1D1A1B07049173) and by the Korea government (MSIT) (No. NRF-2018R1A5A1024127). The authors are grateful for the supports.

***Corresponding Author:** Young Seok Song (ysong@dankook.ac.kr)

2. Experimental

2.1. Materials and preparation of fiber reinforced thermoplastics

The pellets were prepared *via* the pultrusion process and then injection-molded. Two different lengths of the pellets, 11 and 3 mm were considered in this study. Polypropylene (PP) was used as a matrix, and glass and carbon fibers were employed as a filler for the composites. The loading of glass fiber was ranged from 20 to 50 wt%, and the carbon fiber was loaded by 20 to 40 wt% (Lotte Chemical, LFT). The samples were fabricated using the plunger- and screw-type injection molding processes.

2.2. Measurements

To analyze the length of fiber in the composites, the specimens were burned using a furnace. A three-point bending test was conducted using a universal testing machine (UTM, UTM3365 Instron). The thermal property of the pellets was analyzed using differential scanning calorimetry (DSC, DSC4000 Perkin Elmer) and thermogravimetric analysis (TGA, TGA2950 TA instruments). The specimens for the DSC were scanned from 30 to 250 °C at a heating rate of 20 °C/min. The samples for the TGA were heated from 30 to 600 °C at a heating rate of 20 °C/min. The simple shear test and oscillatory test were conducted in order to characterize the rheological properties of the samples. The measurements were conducted using a rheometer (MCR302 Anton-Paar) with a 25 mm parallel plate at 210 °C. The morphological characteristics were confirmed by scanning electron microscopy (SEM, S-4700 Hitachi) and micro-computed tomography (μ-CT, Skyscan1172 Skyscan). The mold filling and fiber orientation in the composites were numerically modeled using a commercial software, Moldex3D. For this, a mold cavity with a dog-bone shape 40 wt% long glass fiber embedded PP were taken into account. The numerical results were compared with the experimental data.

3. Results and discussion

3.1. Thermal property

Figure 1 shows the TGA and differential thermogravimetric (DTG) curves of the samples. The long glass fiber (LGF) incorporated PP pellets were produced *via* the pultrusion process. The thermal decomposition behavior was analyzed with respect to the fiber loading. In the DTG curve, only one peak was identified. On the other hand, the melting temperature of glass is over 700 °C. Thus, it was inferred that that the degradation occurred due to a single reaction of only PP. As the content of fiber was increased, the resulting peak became sharper in the DTG graph moved towards high temperature. That is, the thermal property was improved with increasing the fiber loading.

Figure 2 presents the DSC curves of the LFTs. Compared with the pure PP, the LGF reinforced composites showed relatively low melting temperature. The addition of glass fibers led to a

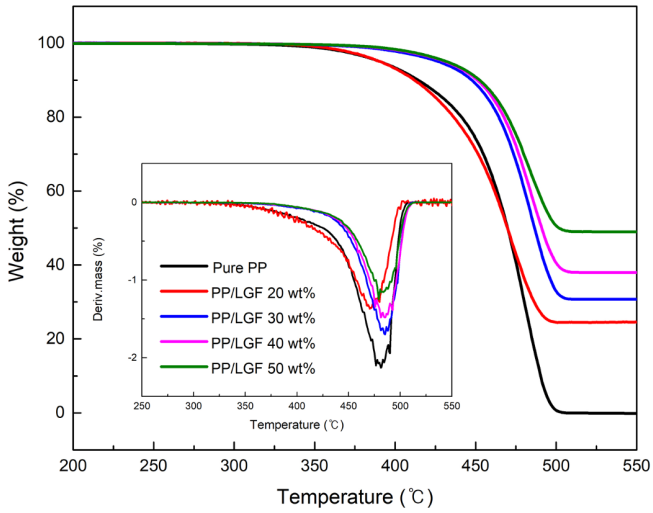

Figure 1. TGA and DTG curves of the specimens.

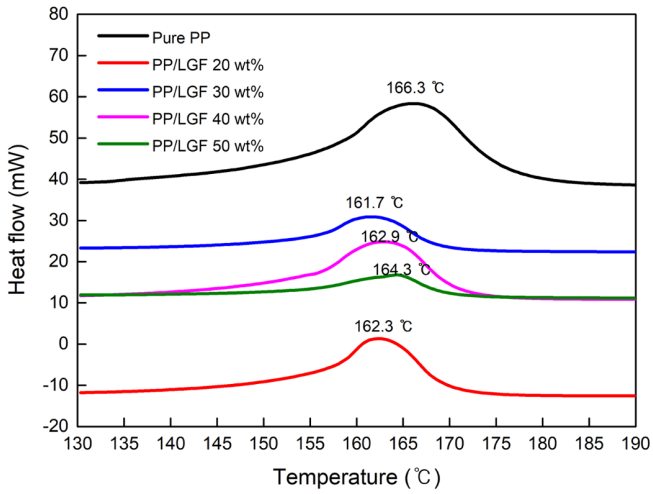

Figure 2. DSC results of the composites.

decrease in the melting temperature, which was because of the reduction of the crystallinity of PP induced by the incorporation of glass fibers. However, the trend of the decrement in the melting temperature according to the weight percentage of fiber was not clear. This might be because the composites were not sufficiently homogenous.

3.2. Rheological property

The shear viscosity of the pellets is shown in Figure 3. As the fiber content increased, the shear viscosity and the shear thinning behavior increased. When shear stress is applied, the hydrodynamic resistance decreases because of the orientation of macromolecules and fillers along the shear flow direction. Such an effect becomes larges as the weight percent of the fibers increases.[21] The viscoelastic materials also show time-dependent rheological properties. To look into this in a more controlled manner, we carried out the oscillatory shear test.

Figure 4 shows the results of the oscillatory test at a fixed temperature. According to the Cox-Merz rule, the values of the complex viscosity and the shear viscosity are equal at the same values of frequency and shear rate, respectively: $\eta(\dot{\gamma}) =$

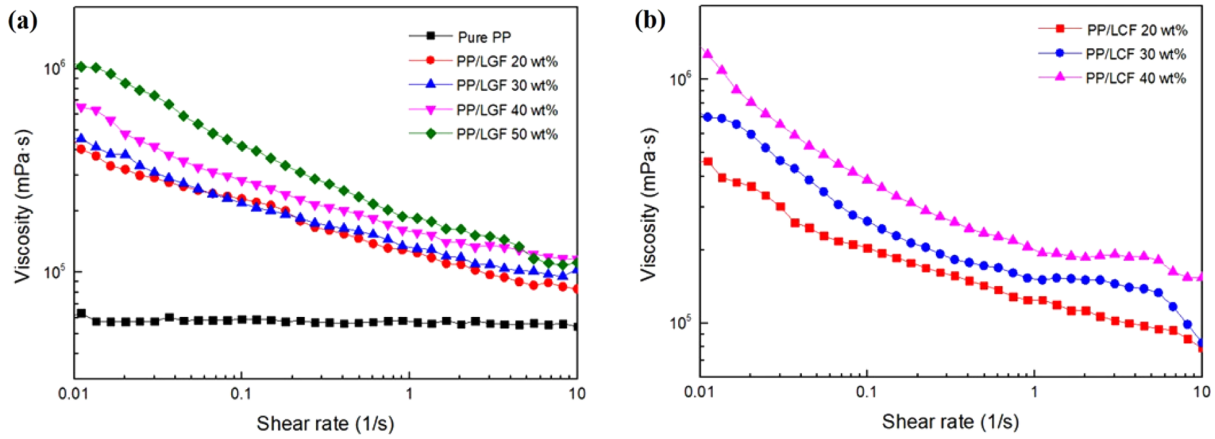

Figure 3. Shear viscosity of the pellets with respect to the shear rate at 210 °C: (a) Long glass fiber reinforced thermoplastics and (b) long carbon fiber reinforced thermoplastics.

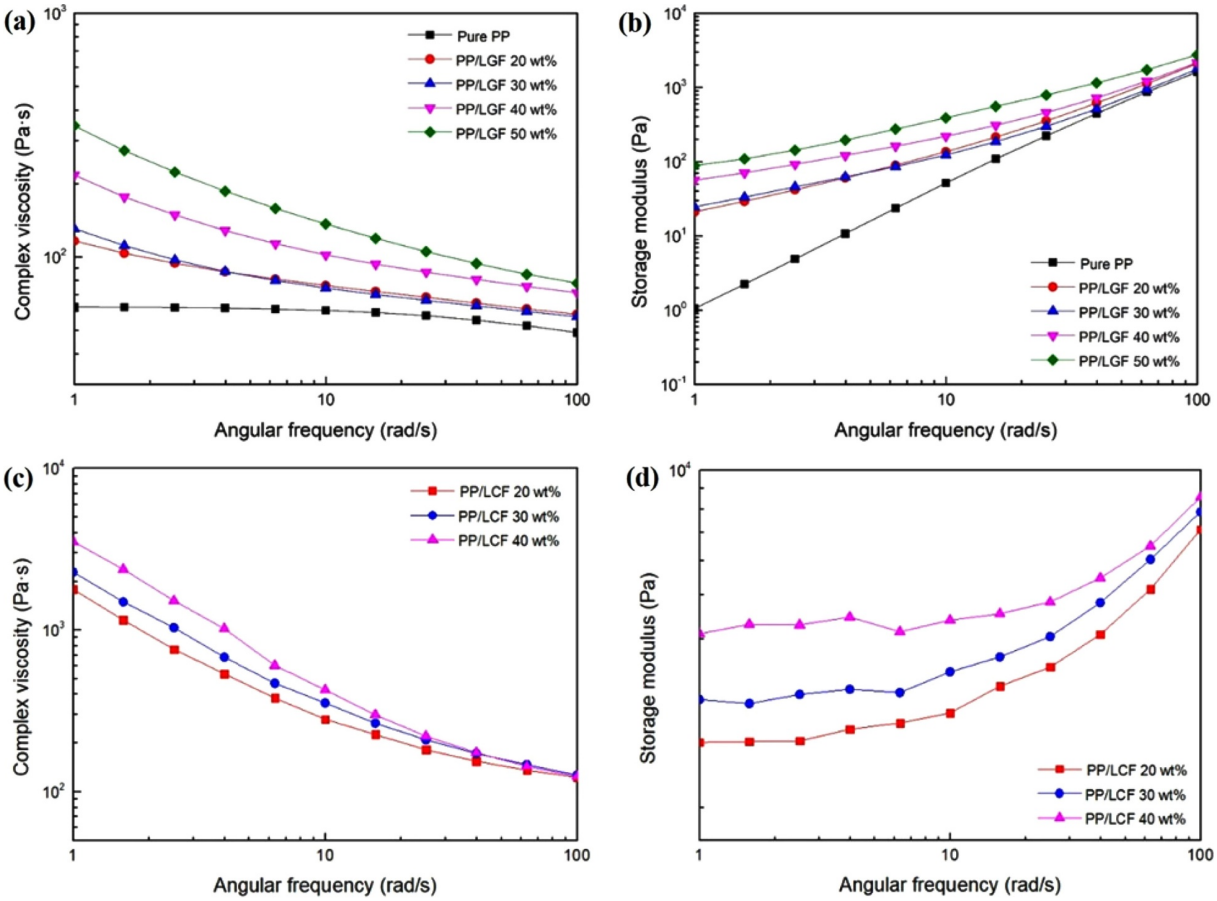

Figure 4. Results of oscillatory shear test for the composites. (a) Complex viscosity and (b) storage modulus of the long glass fiber composites. (c) Complex viscosity and (d) storage modulus of the long carbon fiber composites.

$|\eta^*(\omega)|_{\omega=\dot{\gamma}}$. However, the composites handled in this study were found not to follow the rule as shown in Figure 4(a) and (c). Interestingly, the complex viscosity of the carbon fiber reinforced thermoplastics was higher than that of the glass fiber reinforced composites. This was due to the fact that the carbon fiber has higher Young's modulus than the glass fiber. As shown in Figure 4(b) and (d), the storage moduli increased with increasing the content of the fiber. If the interaction between the filler and the matrix increases, the storage modulus increases. In addition, As the glass fiber loading increased, the slope of the storage modulus decreased (Figure 4(b)).[22] The decreasing slope means that the samples exhibit a behavior similar to an elastic solid. When a constant stress is applied to a viscoelastic material, resulting modulus decreases over time. This is due to the fact that the materials undergo molecular rearrangement in order to minimize local stress. Thus, the modulus measured at a high frequency (*i.e.*, for a short time) is relatively high compared with that measured at a low frequency (*i.e.*, for a long time).

Tables 1 and 2 list the power law indices and yield stresses of the LGF and LCF composites, respectively. The power law model

Table 1. Power-law index and yield stress of long glass fiber composites

wt% of glass fiber	Power-law index (n)	Yield stress
50 wt%	0.7128	2.2665
40 wt%	0.7375	2.1744
30 wt%	0.7426	2.1396
20 wt%	0.7599	2.1593
0 wt%	0.9925	1.4471

Table 2. Power-law index and yield stress of long carbon fiber composites

wt% of carbon fiber	Power-law index (n)	Yield stress
50 wt%	-	-
40 wt%	0.6382	2.3425
30 wt%	0.7445	2.2841
20 wt%	0.7800	2.1719
0 wt%	0.9925	1.4471

assumes that $\tau = K\dot{\gamma}^n$, where τ is the shear stress, $\dot{\gamma}$ is the shear rate, and K is a constant. The power law index was calculated through linear regression analysis. As the power law index increases, the shear thinning effect is increased. This may imply an improvement in the processability because the melt viscosity is decreased during processing. The yield stress was determined by extrapolating the shear viscosity data. The deformation is closely related to the yield stress. As the fiber loading increased, the yield stress increased. The yield stress of the long carbon fiber reinforced thermoplastics was larger than that of the long glass fiber reinforced thermoplastics.

3.3. Length distribution of glass fiber

The long glass fiber length of the composites was analyzed experimentally. Figure 5(a) shows the length distribution of fiber in the composite prepared *via* the plunger-type injection molding process. It was found that most of the fibers maintained their initial length after molding. However, the fiber length of the composite fabricated through the screw-type injection molding was reduced by more than half due to the screw motion (Figure 5(b)). The fiber length and its distribution play a critical role in the mechanical properties. Even if the filler damage by the screw is very severe, it is hard to completely avoid the problem during processing.

3.4. Mechanical property

The three-point bending test was conducted using a UTM. The flexural strength and modulus of the samples are presented in Figure 6. First, the flexural strength increased with an increase

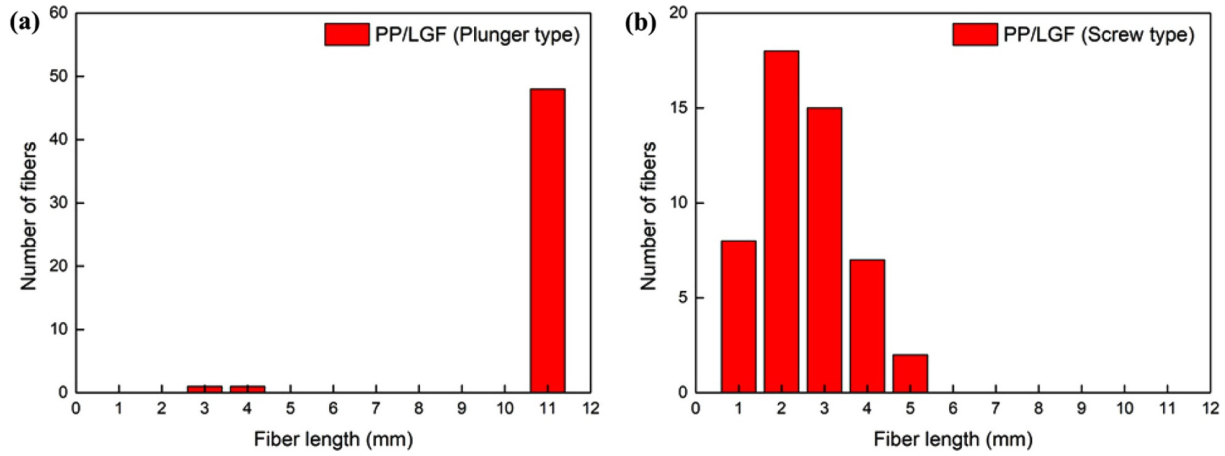

Figure 5. Length distributions of the long glass fiber in the composites prepared using (a) plunger-type injection-molding and (b) screw-type injection-molding.

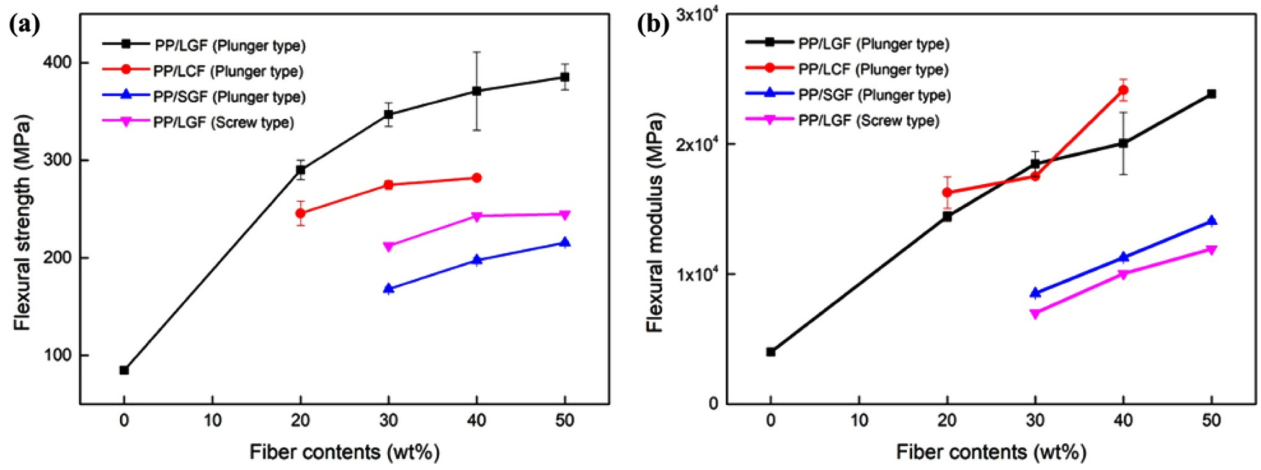

Figure 6. Results of the three-point bending test for the specimens: (a) Flexural strength and (b) flexural modulus.

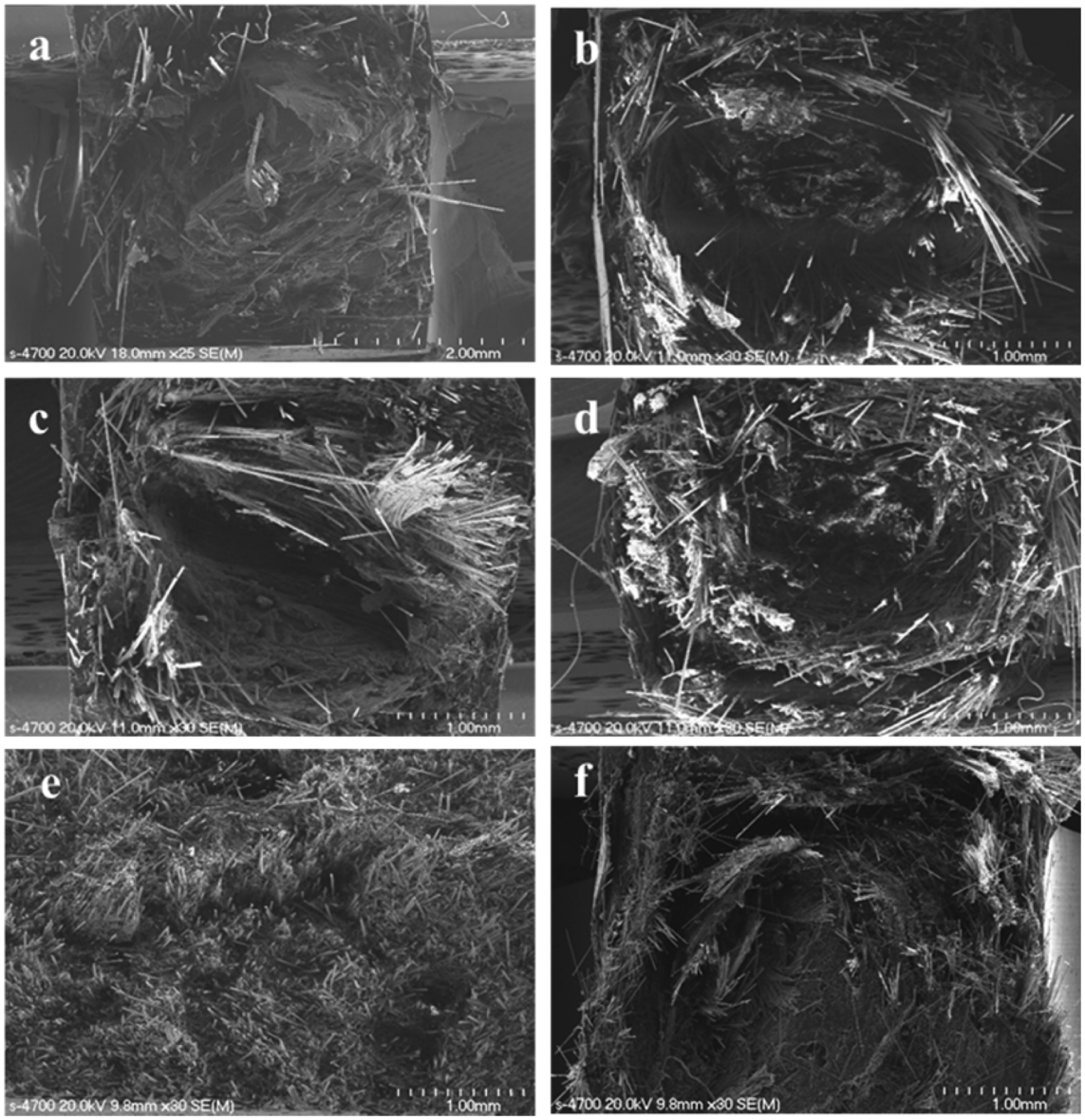

Figure 7. Cross-sectional FESEM images: (a) PP/LGF 20 wt% composite, (b) PP/LGF 30 wt% composite, (c) PP/LGF 40 wt% composite, (d) PP/LGF 50 wt% composite prepared *via* plunger-type injection molding, (e) PP/LGF 40 wt% composite prepared *via* screw-type injection molding, and (f) PP/SGF 40 wt% composite prepared *via* plunger type injection molding.

in wt% of the fiber. As expected, the LGF composites prepared *via* the plunger-type injection molding had the highest strength. The LGF composites produced using the screw type injection-molding process possessed somewhat similar values to the SGF composites. This was attributed to the fact that long glass fibers were cut. In the case of the strength, the contribution of the fiber length is critical but the modulus of composites mostly depends on the volume fraction of the filler. The effect of the fiber content on the modulus was more significant than on the strength (Figure 6(b)).

3.5. Morphological property

Figure 7 presents the cross-sectional images of the composites after being fractured. It was found that many of the fibers were pulled out across the cross-section. Furthermore, the fibers were oriented along the flow direction forming a cylindrical shell. This is the so-called skin-shear-core structure of injection molded parts. At the skin zone, since the amount of time is not sufficient to orient the fillers due to the rapid solidification of the molten polymer onto the mold wall, the fillers are not oriented in a specific direction. However, the fillers are orientated well at the shear zone by the high shear stress. The fillers at the core zone tend to show random orientation again. The portion of the skin, shear, and core zones are associated with injection-molding conditions such as mold temperature, flow rate and pressure. The fiber orientation was also analyzed numerically. Figure 8(a) shows the fiber orientation on the skin, and Figures 8(b), (c), and (d) show the fiber orientation at the cross-section along the *x*, *y*, and *z* directions, respectively. Here, the y-direction indicates the main flow direction, *i.e.*, longitudinal direction.

CT is a device that continuously takes X-rays of a subject while penetrating radiation from various angles in order to obtain the radiation absorption from a cross-section of a specimen and

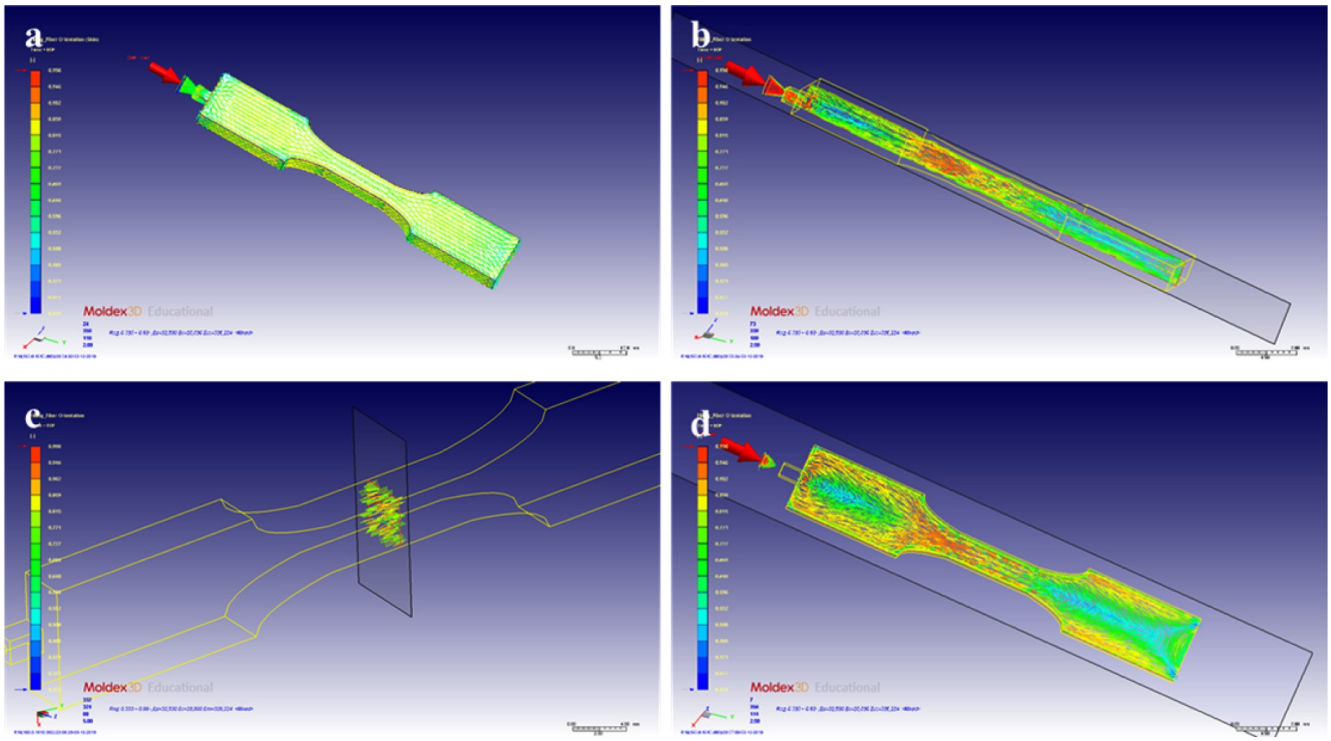

Figure 8. Simulation results of fiber orientation for the composites: (a) Skin layer, (b) y-z plane, (c) x-z plane, and (d) x-y plane.

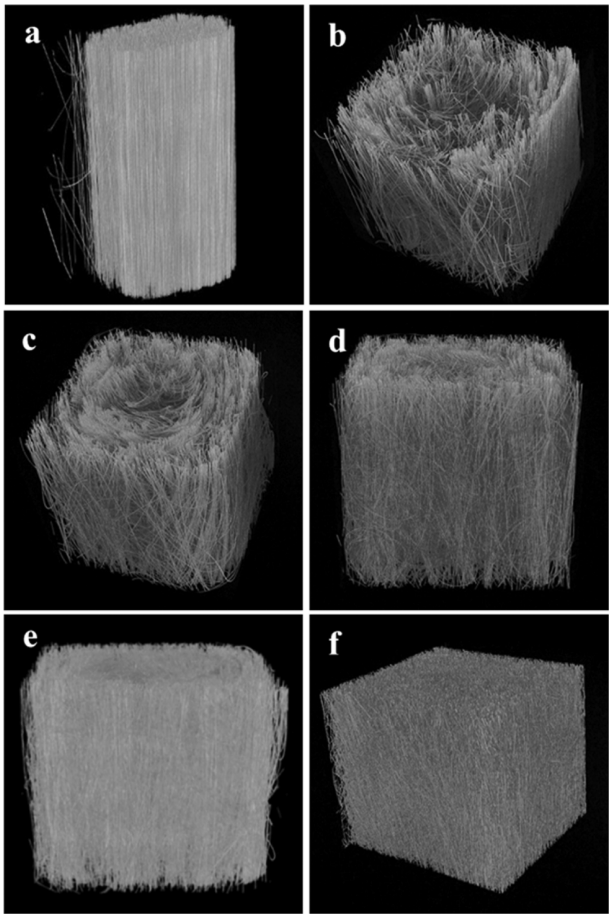

Figure 9. 3D images of micro-CT: (a) Pellet when a 3 um pixel size was selected, (b) PP/LGF 20 wt% composite when a 10 um pixel size was chosen, (c) PP/LGF 30 wt% composite, (d) PP/LGF 40 wt% composite, (e) PP/LGF 50 wt% composite, and (f) PP/SGF 40 wt% composite prepared *via* plunger-type injection molding.

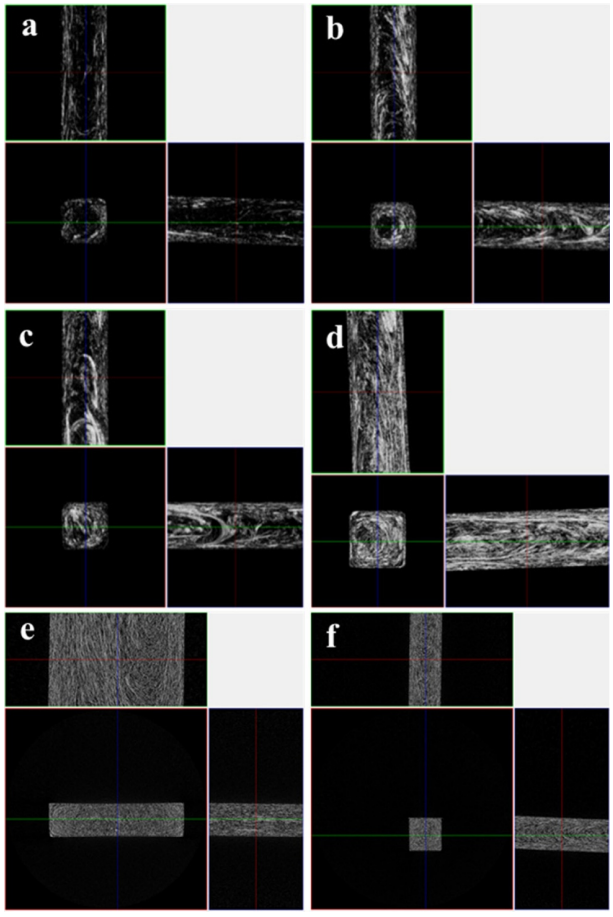

Figure 10. 2D images of micro-CT when a 10 um pixel size was chosen: (a) PP/LGF 20 wt% composite, (b) PP/LGF 30 wt% composite, (c) PP/LGF 40 wt% composite, (d) PP/LGF 50 wt% composite prepared *via* plunger-type injection molding, (e) PP/LGF 40 wt% prepared *via* screw-type injection molding, and (f) PP/SGF 40 wt% prepared *via* plunger-type injection molding.

reconstruct the difference using a computer. In this process, dozens of X-ray cross-sectional images are stacked. The utilization area of CT is very wide, and especially used to diagnose diseases by photographing biomaterials such as bone and teeth. The main advantage of CT is that it can take 3D images without disturbing the specimens. Micro-CT (μ-CT) takes pictures with a micro-pixel size and can closely observe microunits with high-resolution images for internal structure.[23-26] In this study, μ-CT was used to identify the overall fiber orientation of the composites. Figures 9 and 10 demonstrate the 3D and 2D images of the μ-CT for the samples, respectively. The internal structure of the composites was investigated using different pixel sizes, 3 and 10 μm. Figure 9(a) shows the 3D images of the pellets prior to injection molding. The long fibers were found to be oriented in the vertical direction. The results confirmed that the fibers were not cut off during the plunger type injection-molding. The longer fibers were more orientated along the flow direction than the short fibers. Similar to the results of the FEM analysis, the skin-core-shell structure was formed by the fibers in the composites. As a result of the shear stress by the screw during injection molding, the long fibers were broken and shortened. Those results revealed that the experimental observation was in a good agreement with the numerical result.

4. Conclusions

We fabricated LFT and SFT using different injection molding methods and analyzed their physical properties. Also, different kinds of fiber, i.e., glass fiber and carbon fiber were considered for the composites. The mechanical properties of the LFT were better than those of the SFT. As expected, the mechanical and thermal properties were improved with increasing the content of the filler. The carbon fiber reinforced composites showed slightly higher modulus and viscosity than the glass fiber reinforced composites, but the difference was not that significant. In addition, the plunger- and screw-type injection molding samples were compared. The long fibers embedded in the composites were damaged during the screw-type injection molding, and the resulting properties were similar to those of the SFT. The fiber orientation was experimentally observed through μ-CT and SEM analyses, and numerically calculated. This study is expected to provide more comprehensive understanding about fiber reinforced composites fabricated *via* injection molding.

References

(1) D. G. Seong, C. Kang, S. Y. Pak, C. H. Kim, and Y. S. Song, *Compos. Part B: Eng.*, **168**, 218 (2019).
(2) J. Thomason, *Compos. Part A: Appl. Sci. Manuf.*, **36**, 995 (2005).
(3) J. Thomason, *Compos. Part A: Appl. Sci. Manuf.*, **33**, 1641 (2002).
(4) J. Thomason and M. Vlug, *Compos. Part A: Appl. Sci. Manuf.*, **27**, 477 (1996).
(5) J. Thomason and M. Vlug, *Compos. Part A: Appl. Sci. Manuf.*, **28**, 277 (1997).
(6) J. Thomason, M. Vlug, G. Schipper, and H. Krikor, *Compos. Part A: Appl. Sci. Manuf.*, **27**, 1075 (1996).
(7) D. Zhang, M. He, S. Qin, J. Yu, J. Guo, and G. Xu, *Polym. Compos.*, **39**, 63 (2018).
(8) Y. Arao, S. Yumitori, H. Suzuki, T. Tanaka, K. Tanaka, and T. J. C. P. A. A. S. Katayama, *Compos. Part A: Appl. Sci. Manuf.*, **55**, 19 (2013).
(9) D. G. Papageorgiou, I. A. Kinloch, and R. J. Young, *Compos. Sci. Technol.*, **137**, 44 (2016).
(10) W. Xiaoyin, L. Xiandong, S. Yingchun, W. Xiaofei, L. Wanghao, and P. Yue, *Proc. Inst. Mech. Eng. C J. Mech. Eng. Sci.*, **230**, 1634 (2016).
(11) Y.-J. Yim, K.-M. Bae, and S.-J. Park, *Macromol. Res.*, **26**, 794 (2018).
(12) S. H. Lee, J. Y. Kim, C. M. Koo, and W. N. Kim, *Macromol. Res.*, **25**, 936 (2017).
(13) K. Friedrich, in *AIP Conference Proceedings*, AIP Publishing, **1736**, 20001 (2016).
(14) G. Colucci, H. Simon, D. Roncato, B. Martorana, and C. Badini, *J. Thermoplastic Compos. Mater.*, **30**, 707 (2017).
(15) M. Tomioka, T. Ishikawa, K. Okuyama, and T. Tanaka, *J. Compos. Mater.*, **51**, 3847 (2017).
(16) I. Baran, J. H. Hattel, and R. Akkerman, *Compos. B Eng.*, **68**, 365 (2015).
(17) H. Teodorescu-Draghicescu, S. Vlase, M. D. Stanciu, I. Curtu, and M. Mihalcica, *Mater. Plast.*, **52**, 62 (2015).
(18) J. H. Phelps, A. I. A. El-Rahman, V. Kunc, and C. L. Tucker, III, *Compos. Part A: Appl. Sci. Manuf.*, **51**, 11 (2013).
(19) J. Azenha, M. Gomes, P. Silva, and A. J. Pontes, *Polym. Eng. Sci.*, **58**, 560 (2018).
(20) J. Wang, Q. Mao, and J. Chen, *J. Appl. Polym. Sci. Symp.*, **130**, 2176 (2013).
(21) R. Hsissou and A. Elharfi, *J. King. Saud. Univ. Sci.*, **32**, 235 (2020).
(22) R. Hsissou, M. El Bouchti, and A. Elharfi, *J. Mater. Environ. Sci.*, **8**, 12 (2017).
(23) H. Cochard, S. Delzon, and E. Badel, *Plant. Cell. Environ.*, **38**, 201 (2015).
(24) S. J. Schambach, S. Bag, L. Schilling, C. Groden, and M. A. Brockmann, *Methods*, **50**, 2 (2010).
(25) K. Schladitz, *J. Microsc.*, **243**, 111 (2011).
(26) S. H. Hwang, D. J. Lee, H. R. Youn, Y. S. Song, and J. R. Youn, *Macromol. Res.*, **23**, 844 (2015).